Proceedings of the IASS 2024 Symposium
Redefining the Art of Structural Design
August 26-30, 2024, Zurich Switzerland
Philippe Block, Giulia Boller, Catherine DeWolf,
Jacqueline Pauli, Walter Kaufmann (eds.)

On improving buckling resistance in structural topology optimization

Tao XU[a], Xiaodong HUANG[b], Xiaoshan LIN[a], Yi Min XIE[a,*]

[a,*] Centre for Innovative Structures and Materials, School of Engineering, RMIT University
Melbourne 3001, Australia
mike.xie@rmit.edu.au

[b] School of Engineering, Swinburne University of Technology

Abstract

Topology optimization is increasingly becoming an important tool for designing high-performance and light-weight structures. A key challenge is preventing buckling, especially in slender members that are prone to collapsing under pressure. This study introduces techniques to enhance buckling resistance, focusing on two approaches: bi-directional evolutionary structural optimization (BESO) and floating projection topology optimization (FPTO). The numerical examples verify the efficiency of these approaches and underscore the importance of considering buckling in the design process. Both BESO and FPTO are proven to be effective in solving buckling-constrained problems, with FPTO being particularly adept at maximizing buckling strength.

Keywords: topology optimization, buckling resistance, structural design, stability.

1. Introduction

In the last few decades, topology optimization has ascended to a pivotal role in structural engineering, enabling the ideation and realization of structures that are not only high-performing but also material-efficient. Initially, the primary focus of topology optimization was on minimizing structural compliance [1–3]. Over time, the discipline has evolved to embrace a wider range of engineering principles such as natural frequency [4], enhancing stress control mechanisms [5–7], navigating structural complexity [8–9], and facilitating additive manufacturing processes [10–11].

A significant challenge in topology optimization is its tendency to create slender structural elements vulnerable to buckling. This necessitates the incorporation of buckling resistance as a key consideration within topology optimization frameworks to ensure structural safety. However, the consideration of buckling constraints in topology optimization often leads to the occurrence of pseudo buckling modes in intermediate-density elements. These modes cannot accurately reflect true buckling behavior, thereby posing a risk of misinterpreting the structure's stability. The emergence of pseudo buckling modes is attributed to the use of conventional material interpolation schemes with penalization, which reduces the efficiency of intermediate-density elements.

Numerous strategies have been devised to address the challenge of pseudo buckling modes in topology optimization. Neves et al. [12] proposed a technique to cut off the stress stiffness in low-density elements, effectively removing their contribution to the buckling response. Bendsøe and Sigmund [13] introduced a novel approach using two separate material interpolation schemes for calculating stiffness and stress stiffness matrices. Gao and Ma [14] created a process for detecting and eliminating these modes based on the modal strain energy. Recently, Zhang et al. [15] presented an approach based on

constructing matrices that allocate minimal pseudo masses to freedoms encircled by low-density elements.

Considering the abovementioned challenges, two innovative buckling topology optimization methods based on bi-directional evolutionary structural optimization (BESO) and the floating projection topology optimization (FPTO) method have been developed. The BESO method, which categorizes design variables into only solid or void states, naturally circumvents the issue of pseudo buckling modes in intermediate-density elements [16]. The FPTO method allows the use of the linear material interpolation scheme, which can eliminate pseudo buckling modes by avoiding the scaling down of intermediate-density elements [17, 18].

In this study, the capabilities of the BESO and FPTO methods in addressing buckling optimization problems are investigated. Specifically, the study explores the buckling load factor (BLF) maximization and buckling-constrained problems. The results showcase the exceptional convergence properties of both methods, underscoring their efficacy in structural optimization.

This paper is organized as follows: Section 2 introduces the optimization algorithms, including the problem statement, buckling analysis formulas, and the optimization process. Section 3 presents two numerical examples to illustrate the effectiveness and robustness of the algorithms. Conclusions are provided in Section 4.

2. Optimization algorithms

This section delves into the optimization algorithms employed in this study, detailing the problem statement, the essential formulas for buckling analysis, and the optimization procedures.

2.1 Problem statement

The mathematical model for topology optimization for maximizing the critical BLF is formulated as

$$\begin{aligned} &\max: \lambda_1 \\ &\text{s.t.:} \begin{cases} \mathbf{F} = \mathbf{K}\mathbf{U} \\ V_f = \dfrac{\sum_e x_e V_e}{\sum_e V_e} \le V_f^* \\ x_{min} \le x_e \le 1 \end{cases} \end{aligned} \tag{1}$$

where λ_1 is the critical BLF. $\mathbf{F}$ is the load applied to the structure. $\mathbf{K}$ and $\mathbf{U}$ are the global stiffness matrix and the displacement vector, respectively. V_f and V_f^* denote the volume fraction of the structure and its constraint value. x_e (e = 1, 2, ...) is the design variable, and V_e is the volume of the corresponding element. x_{min} is a minimal positive value, e.g., 10^{-3} to 10^{-9}, to avoid the singularity. For the discrete BESO method, x_e is the binary design variable, which equals either x_{min} (void) or 1 (solid).

The buckling-constrained topology optimization is modeled as

$$\begin{aligned} &\min: C = \frac{1}{2}\mathbf{U}^T\mathbf{K}\mathbf{U} \\ &\text{s.t.:} \begin{cases} \mathbf{F} = \mathbf{K}\mathbf{U} \\ V_f = \dfrac{\sum_e x_e V_e}{\sum_e V_e} \le V_f^* \\ \lambda_1 \ge \underline{\lambda} \\ x_{min} \le x_e \le 1 \end{cases} \end{aligned} \tag{2}$$

where C is the mean compliance, and $\underline{\lambda}$ denotes the predetermined buckling constraint.

2.2 Buckling analysis

To enhance computational efficiency, this study utilizes the linear buckling analysis, expressed as

$$(\mathbf{K}+\lambda_i\mathbf{G})\mathbf{\Phi}_i=0 \tag{3}$$

where λ_i is the i-th BLF, and $\mathbf{\Phi}_i$ denotes the corresponding buckling mode vector. The global stress stiffness matrix, **G**, is assembled from the element stress stiffness matrix, as shown in Eq. (3).

$$\mathbf{G}_e=\mathbf{B}_g^T\mathbf{S}\mathbf{B}_g \tag{4}$$

where $\mathbf{B}_g$ signifies the derivatives of the shape function. **S** is the matrix assembled from the stress components.

2.3 Optimization workflow

The optimization process for both the buckling-constrained BESO and FPTO methods is illustrated in Figures 1 and 2, respectively, via detailed flowcharts.

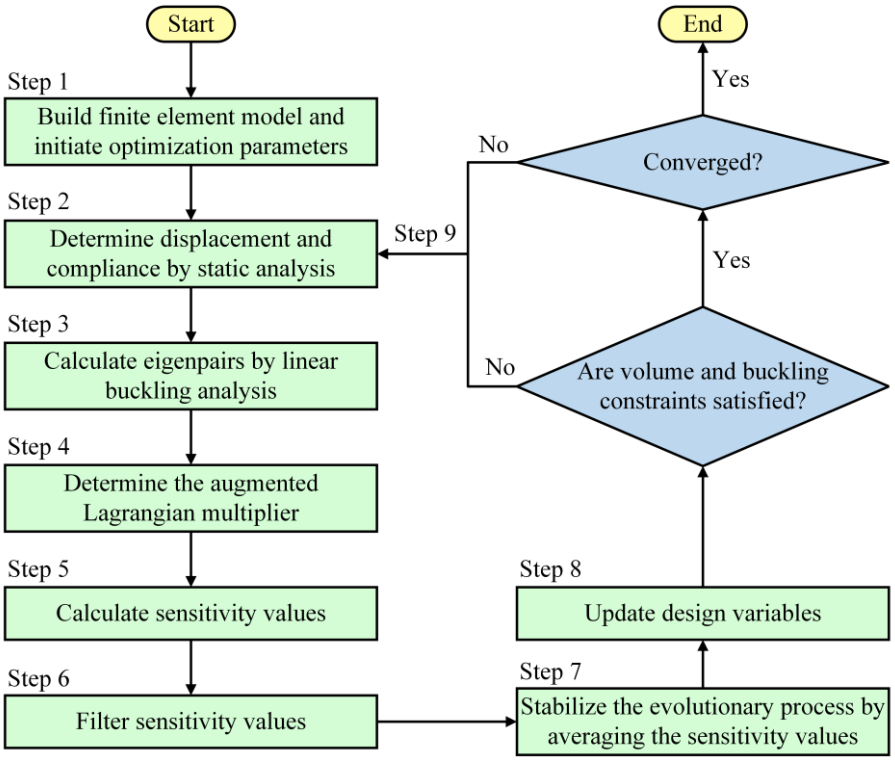

Figure 1. Flowchart of the buckling-constrained BESO method.

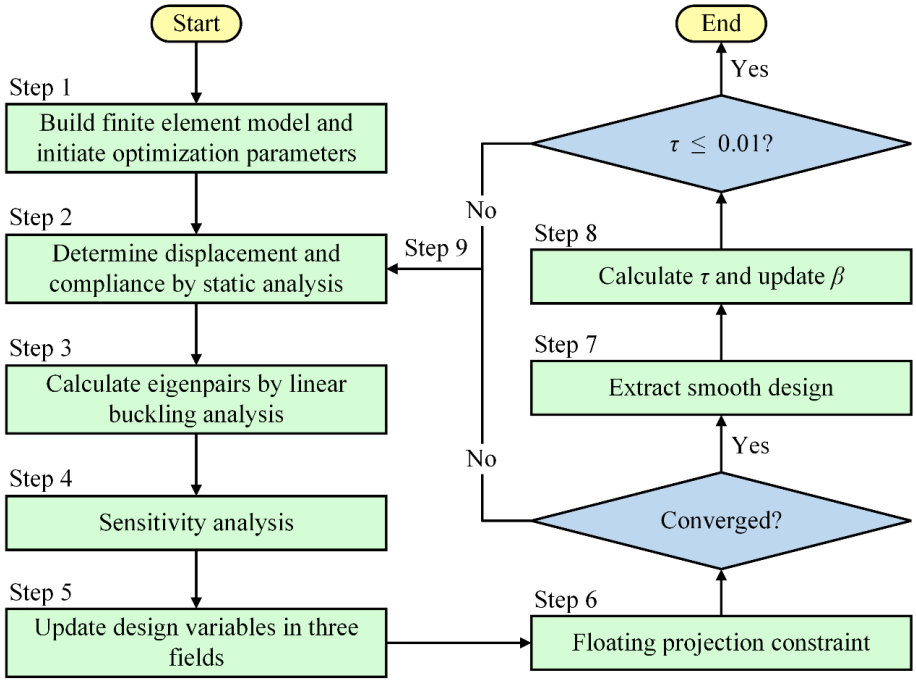

Figure 2: Flowchart of the buckling-constrained FPTO method.

3. Numerical examples

This section presents two numerical examples to showcase the efficacy of both the BESO and FPTO algorithms. The selected examples illustrate the optimization challenges and solutions in two distinct scenarios: BLF maximization and buckling-constrained problem. The performance of the BESO and FPTO methods is evaluated and compared based on the results obtained from these examples.

In all numerical examples, plane stress elements are utilized. Young's modulus and Poisson's ratio are set as $E = 1$ and $v = 0.3$, respectively.

3.1 BLF maximization for a compressed column

Buckling is a common issue in structural components subjected to compression, particularly in slender members. This example focuses on maximizing the critical BLF in a compressed column, as depicted in Figure 3. The rectangular design domain with dimensions $L_x = L_y/2 = 1$ is discretized into 240×480 elements. A downward force of magnitude $F = 1\times10^{-3}$ is uniformly applied at the top across a length of $l/L_x = 1/15$. Beneath the applied force, an area with a depth of $l/2$ is designated as the non-design domain, while the bottom of the design domain is fixed.

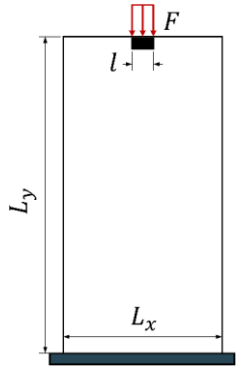

Figure 3. Design domain and boundary conditions of the compressed column.

The target volume fraction is set at $V_f^* = 25\%$, and the filter size r_{min} = 4×the element side length. The optimization process using the BESO method is shown in Figure 4. The optimization using the BESO

method begins with a stiffness design that takes the shape of a simple column (Figure 4a). As the optimization progresses, the column evolves into two bars connected by thin cross-like members (Figure 4b–4e). The first BLF (λ_1) improves from 0.89 in the initial column to 9.21 in the final design (Figure 4f).

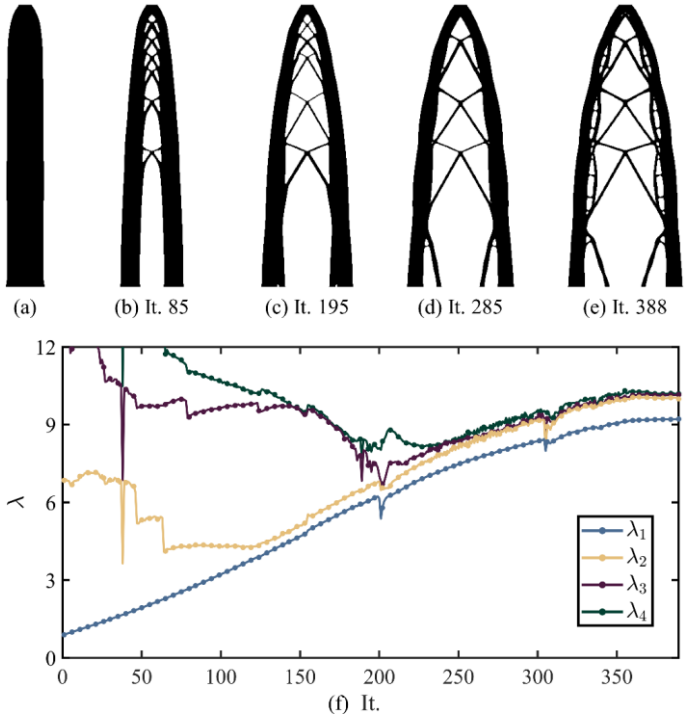

Figure 4. BESO optimization process: (a) initial stiffness design; (b–e) structural topologies at different iterations; and (f) evolutionary histories of the first four BLFs [16].

In contrast, the FPTO method starts from a full design domain without a predefined stiffness design, as shown in Figure 5. Initially, two bars emerge (Figure 5a), followed by the transformation of grey elements into cross-like members (Figure 5b–5d). The final design achieves a critical BLF of 11.63, 30.0% higher than the BESO method.

Comparing the methods reveals that the result obtained with the BESO method depends on the initial stiffness design, while the FPTO method, independent of such stiffness design, achieves a significantly higher critical BLF. However, the FPTO method requires over 1,500 iterations to converge to a binary 0/1 design, contrasting with the faster convergence of the BESO method with 388 iterations. Both methods effectively mitigate pseudo buckling modes and demonstrate stable optimization processes (Figure 4f and 5e).

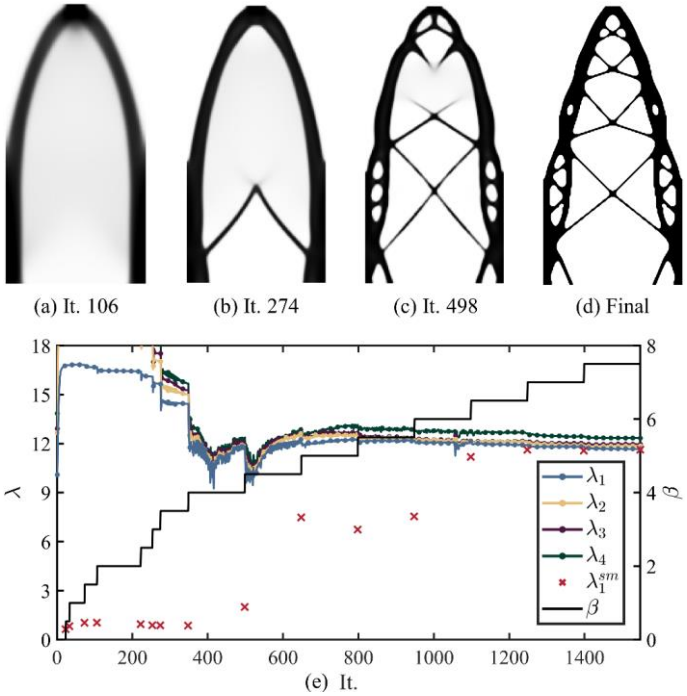

Figure 5. FPTO optimization process: (a–c) structural topologies at different iterations; (d) final smooth design [18]; and (e) evolutionary histories of the first four BLFs. Note that histories of λ_1–λ_4 marked with different colors are BLFs of the element-based design, and the red crosses represent the critical BLF of the smooth designs.

3.2 Buckling-constrained optimization for a frame structure

This section addresses the buckling-constrained topology optimization problem for a frame structure. The boundary conditions and design domain of the structure are illustrated in Figure 6a, with the domain discretized into 90 × 210 elements. A downward force $F = 2 \times 10^{-2}$ is evenly distributed over a length of $l = b/10$, located at the midpoint of the right side. The left side of the domain is fixed near the upper and lower ends over a length of l.

The target volume fraction V_f^* is set as 20%, with the filter size r_{min} equal to 2×the element side length. The initial stiffness design obtained through the BESO method features symmetric upper and lower bars (Figure 6b), where the lowest BLF $\lambda_1 = 0.89$ suggests buckling susceptibility in the lower bar.

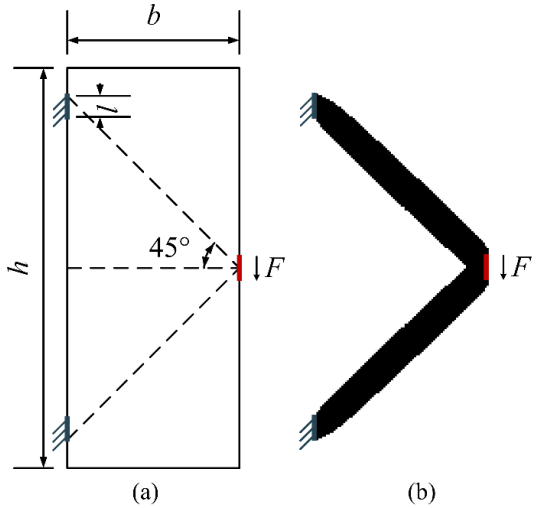

Figure 6. The frame example: (a) design domain and boundary conditions; and (b) the stiffness design obtained by the BESO method.

For optimization with the BESO method, the resultant optimized designs are depicted in Figure 7. The optimization leads to a redistribution of material from the upper bar to the lower bar, which divides into two bars connected by slender elements to enhance buckling resistance. A notable feature is the occurrence of a connecting bar between the upper and lower bars, with its thickness and length increasing alongside the buckling constraint, as highlighted by red circles in Figure 7b–7f. This connecting bar significantly increases the structure's moment of inertia, which is crucial for mitigating rotational movement at the junction.

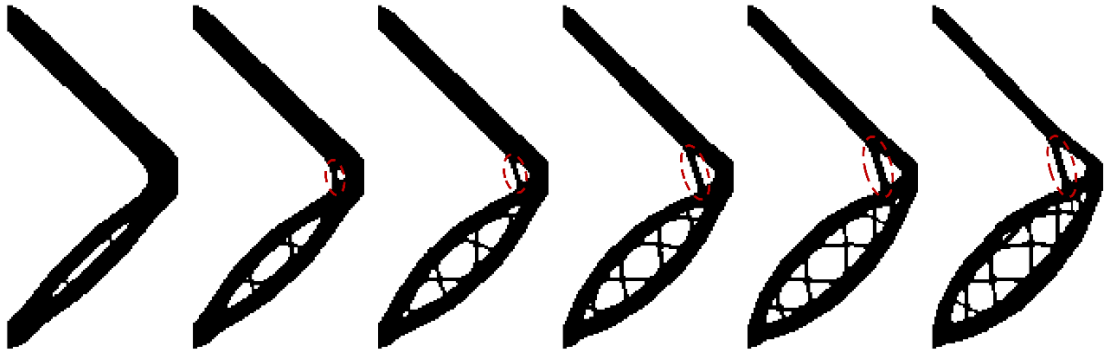

Figure 7. Optimized designs of the two-bar frame using the BESO method [16].

Figure 8 presents the optimized designs using the FPTO method. It can be seen that the optimized results are very similar to that of the BESO method. However, it is noteworthy that the compliance in each design produced by the FPTO method is slightly higher than that obtained with the BESO method.

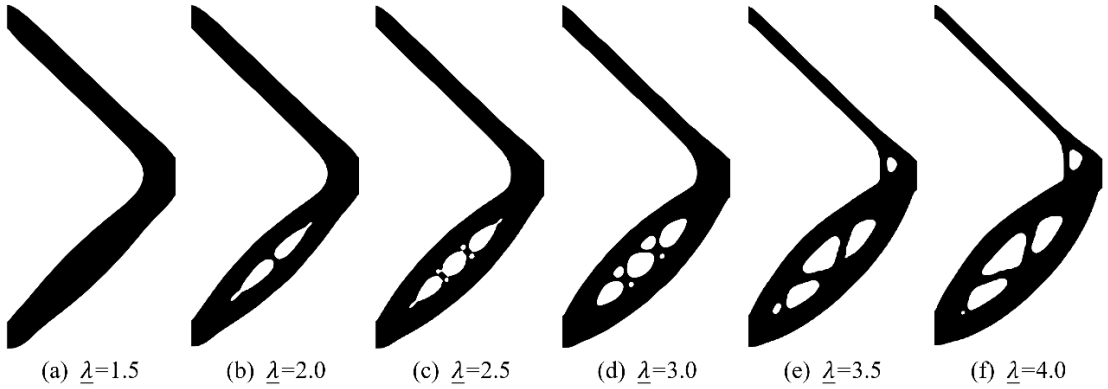

Figure 8. Optimized designs of the two-bar frame using the FPTO method.

Figure 9 shows the comparison of optimization histories for both methods with $\underline{\lambda} = 4.0$. This comparison reveals that both the BESO and FPTO methods exhibit good convergence and satisfy the specified buckling constraints. Nevertheless, the FPTO method requires a higher number of iterations compared to the BESO method.

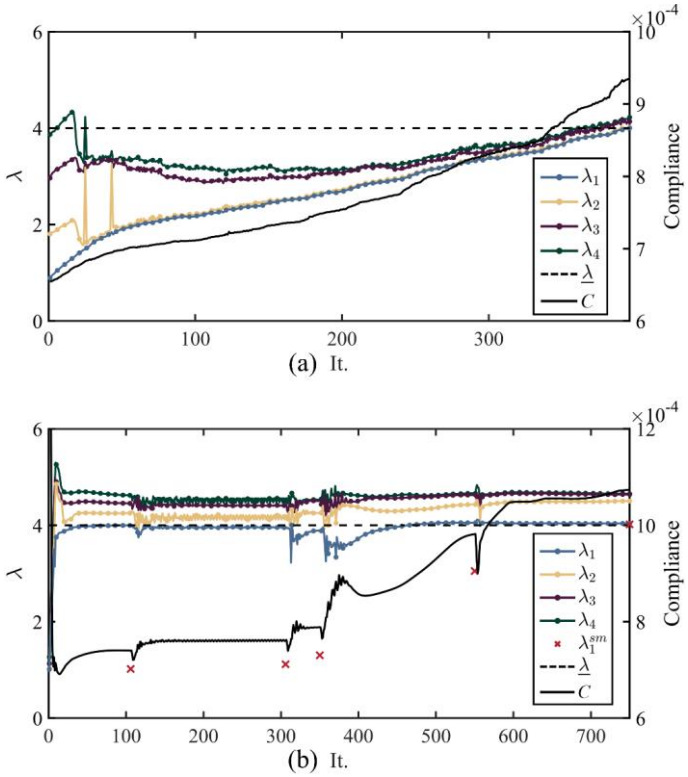

Figure 9. Optimization histories with $\underline{\lambda} = 4.0$ using (a) BESO method and (b) FPTO method.

4. Conclusions

This study delves into topology optimization considering buckling and employs both the BESO and FPTO methods. The effectiveness of these methods in maximizing the buckling load factor and tackling buckling-constrained optimization is demonstrated via two numerical examples. The BESO method offers computational efficiency but produces results that depend on the initial stiffness design, whereas the FPTO method achieves independence from stiffness designs, albeit requiring more iterations for the optimization process. This research highlights the importance of considering buckling in structural design and serves as a valuable guide for architects and engineers in creating efficient and stable structures. For future research, extending the proposed algorithm to 3D examples and including manufacturing constraints are recommended for more practical applications in real-world scenarios.

Acknowledgements

The authors gratefully acknowledge the financial support from the Australian Research Council (FL190100014).

References

[1] M. P. Bendsøe and N. Kikuchi, "Generating optimal topologies in structural design using a homogenization method," *Comput Methods Appl Mech Eng*, vol. 71, no. 2, 1988.

[2] G. I. N. Rozvany, "Difficulties in truss topology optimization with stress, local buckling and system stability constraints," Springer-Verlag, 1996.

[3] Y. M. Xie and G. P. Steven, "A simple evolutionary procedure for structural optimization," *Comput Struct*, vol. 49, no. 5, 1993.

[4] X. Huang, Z. H. Zuo, and Y. M. Xie, "Evolutionary topological optimization of vibrating continuum structures for natural frequencies," *Comput Struct*, vol. 88, no. 5–6, pp. 357–364, Mar. 2010.

[5] O. Amir, "Stress-constrained continuum topology optimization: a new approach based on elasto-plasticity," *Structural and Multidisciplinary Optimization*, vol. 55, no. 5, pp. 1797–1818, May 2017.

[6] A. Chen, K. Cai, Z. L. Zhao, Y. Zhou, L. Xia, and Y. M. Xie, "Controlling the maximum first principal stress in topology optimization," *Structural and Multidisciplinary Optimization*, vol. 63, no. 1, 2021.

[7] C. Le, J. Norato, T. Bruns, C. Ha, and D. Tortorelli, "Stress-based topology optimization for continua," *Structural and Multidisciplinary Optimization*, vol. 41, no. 4, pp. 605–620, Apr. 2010.

[8] Y. He, Z. L. Zhao, X. Lin, and Y. M. Xie, "A hole-filling based approach to controlling structural complexity in topology optimization," *Comput Methods Appl Mech Eng*, vol. 416, 2023.

[9] Y. He, Z. L. Zhao, K. Cai, J. Kirby, Y. Xiong, and Y. M. Xie, "A thinning algorithm based approach to controlling structural complexity in topology optimization," *Finite Elements in Analysis and Design*, vol. 207, Sep. 2022.

[10] M. Bi, P. Tran, and Y. M. Xie, "Topology optimization of 3D continuum structures under geometric self-supporting constraint," *Addit Manuf*, vol. 36, 2020.

[11] M. Bi *et al.*, "Continuous contour-zigzag hybrid toolpath for large format additive manufacturing," *Addit Manuf*, vol. 55, 2022.

[12] M. M. Neves, H. Rodrigues, and M. Guedes, "Generalized topology criterion design of structures with a buckling load," Springer-Verlag, 1995.

[13] M. Bendsøe and O. Sigmund, *Topology optimization. Theory, methods, and applications. 2nd ed., corrected printing*. 2004.

[14] X. Gao and H. Ma, "Topology optimization of continuum structures under buckling constraints," *Comput Struct*, vol. 157, pp. 142–152, Jun. 2015.

[15] G. Zhang, K. Khandelwal, and T. Guo, "Finite strain topology optimization with nonlinear stability constraints," *Comput Methods Appl Mech Eng*, vol. 413, Aug. 2023.

[16] T. Xu, X. Lin, and Y. M. Xie, "Bi-directional evolutionary structural optimization with buckling constraints," *Structural and Multidisciplinary Optimization*, vol. 66, no. 4, p. 67, Apr. 2023.

[17] X. Huang and W. Li, "Three-field floating projection topology optimization of continuum structures," *Comput Methods Appl Mech Eng*, vol. 399, p. 115444, Sep. 2022.

[18] T. Xu, X. Huang, X. Lin, and Y. M. Xie, "Topology optimization for maximizing buckling strength using a linear material model," *Comput Methods Appl Mech Eng*, vol. 417, p. 116437, Dec. 2023.

Proceedings of the IASS 2024 Symposium
Redefining the Art of Structural Design
August 26-30, 2024, Zurich Switzerland
Philippe Block, Giulia Boller, Catherine De Wolf,
Jacqueline Pauli, Walter Kaufmann (eds.)

Copyright Declaration

Before publication of your paper in the Proceedings of the IASS Annual Symposium 2024, the Editors and the IASS Secretariat must receive a signed Copyright Declaration. The completed and signed declaration may be uploaded to the EasyChair submission platform or sent as an e-mail attachment to the symposium secretariat (papers@iass2024.org). A scan into a .pdf file of the signed declaration is acceptable in lieu of the signed original. In the case of a contribution by multiple authors, either the corresponding author or an author who has the authority to represent all the other authors should provide his or her address, phone and E-mail and sign the declaration.

Paper Title: On improving buckling resistance in structural topology optimization

Author(s): Tao Xu, Xiaodong Huang, Xiaoshan Lin, Yi Min Xie

Affiliation(s): RMIT University

Address: Melbourne, Australia

Phone: +61399253655

E-mail: mike.xie@rmit.edu.au

I hereby license the International Association for Shell and Spatial Structures to publish this work and to use it for all current and future print and electronic issues of the Proceedings of the IASS Annual Symposia. I understand this licence does not restrict any of the authors' future use or reproduction of the contents of this work. I also understand that the first-page footer of the manuscript is to bear the appropriately completed notation:

> *Copyright © 2024 by <name(s) of all of the author(s)>*
> *Published by the International Association for Shell and Spatial Structures (IASS) with permission*

If the contribution contains materials bearing a copyright by others, I further affirm that (1) the authors have secured and retained formal permission to reproduce such materials, and (2) any and all such materials are properly acknowledged by reference citations and/or with credits in the captions of photos/figures/tables.

Printed name: Yi Min Xie Signature: 

Location: Melbourne Date: May 26, 2024